

Characterization of Four Covalently-Linked Yeast Cytochrome *c*/Cytochrome *c* Peroxidase Complexes: Evidence for Electrostatic Interaction between Bound Cytochrome *c* Molecules[†]

Siddhartha Nakani, Lidia B. Vitello, and James E. Erman*

Department of Chemistry and Biochemistry, Northern Illinois University, DeKalb, Illinois 60115

Received August 15, 2006; Revised Manuscript Received September 29, 2006

ABSTRACT: Four covalent complexes between recombinant yeast cytochrome *c* and cytochrome *c* peroxidase (rCcP) were synthesized via disulfide bond formation using specifically designed protein mutants (Papa, H. S., and Poulos, T. L. (1995) *Biochemistry* 34, 6573–6580). One of the complexes, designated V5C/K79C, has cysteine residues replacing valine-5 in rCcP and lysine-79 in cytochrome *c* with disulfide bond formation between these residues linking the two proteins. The V5C/K79C complex has the covalently bound cytochrome *c* located on the back-side of cytochrome *c* peroxidase, $\sim 180^\circ$ from the primary cytochrome *c*-binding site as defined by the crystallographic structure of the 1:1 noncovalent complex (Pelletier, H., and Kraut J. (1992) *Science* 258, 1748–1755). Three other complexes have the covalently bound cytochrome *c* located $\sim 90^\circ$ from the primary binding site and are designated K12C/K79C, N78C/K79C, and K264C/K79C, respectively. Steady-state kinetic studies were used to investigate the catalytic properties of the covalent complexes at both 10 and 100 mM ionic strength at pH 7.5. All four covalent complexes have catalytic activities similar to those of rCcP (within a factor of 2). A comprehensive study of the ionic strength dependence of the steady-state kinetic properties of the V5C/K79C complex provides evidence for significant electrostatic repulsion between the two cytochromes bound in the 2:1 complex at low ionic strength and shows that the electrostatic repulsion decreases as the ionic strength of the buffer increases.

Cytochrome *c* peroxidase (CcP¹) is a detoxification enzyme localized between the inner and outer membranes of yeast mitochondria (1). CcP detoxifies hydrogen peroxide by catalyzing its reduction to water using the reducing equivalents from two molecules of ferrocytochrome *c* (2). The catalytic mechanism involves oxidation of the native enzyme by hydrogen peroxide to an oxidized enzyme intermediate followed by reduction of the intermediate back to the native enzyme by ferrocytochrome *c*. CcP effectively couples the two-electron reduction of hydrogen peroxide to the one-electron oxidation of ferrocytochrome *c* by using two equivalents of cytochrome *c* per catalytic cycle. Since

1980, when the 3D structure of CcP was first revealed (3, 4), CcP has played a significant role in elucidating the structural basis for heme protein reactivity, especially in the activation of hydrogen peroxide (5, 6), long-range electron transfer between heme proteins (7, 8), and protein–protein interactions (9, 10).

At low ionic strength, CcP can bind two molecules of cytochrome *c* (11) with quite different affinities. Below 30 mM ionic strength, the binding of the first yeast iso-1 cytochrome *c* is very strong with equilibrium dissociation constants for the 1:1 noncovalent complex, K_{D1} , of less than 0.1 μM (12, 13), whereas binding of the second cytochrome *c* is much weaker with K_{D2} values in the 100 to 200 μM range (7, 14, 15). The ability of CcP to bind more than one molecule of cytochrome *c* had engendered a number of questions concerning the nature of the interaction between these two proteins and the role of cytochrome *c* bound at different locations on the surface of CcP in the catalytic mechanism. We have recently shown that only cytochrome *c* bound in the vicinity of the crystallographically defined (9) or primary binding site is electron transfer active in the normal catalytic cycle of CcP (16). The role of cytochrome *c* binding at secondary sites is only apparent below ~ 100 mM ionic strength and appears to involve the modulation of the rate of association and dissociation of cytochrome *c* from the primary site. This implies interaction between cytochrome *c* molecules bound at the two sites.

[†] This work was supported in part by a grant from the National Institutes of Health (R15 GM59740).

* Corresponding author. Phone: (815) 753-6867. Fax: (815) 753-4802. E-mail: jerman@niu.edu.

¹ Abbreviations: CcP, generic abbreviation for cytochrome *c* peroxidase whatever the source; yCcP, authentic yeast cytochrome *c* peroxidase isolated from *S. cerevisiae*; rCcP, recombinant cytochrome *c* peroxidase expressed in *E. coli*, the rCcP used in this study has an amino acid sequence identical to that of yCcP; mutations in the amino acid sequences of either CcP or cytochrome *c* are indicated by using the one letter code for the amino acid residue in the wild-type protein, followed by the residue number and the one letter code for the amino acid residue in the mutant protein, i.e., C102T represents a mutant in which a threonine residue replaces the cysteine residue at position 102 of the wild-type protein. The four covalent complexes investigated in this manuscript are designated V5C/K79C, K12C/K79C, N78C/K79C, and K264C/K79C, where the first mutational designation is that in rCcP and the second in recombinant yeast iso-1 cytochrome *c* with the disulfide bond linking the two proteins between the two cysteine residues.

In this article, we present the results of steady-state kinetic studies of the catalytic activity of four specifically engineered 1:1 cytochrome *c*/CcP covalent complexes, all of which leave the primary cytochrome *c* binding site open and accessible to free cytochrome *c*. All four covalent complexes are catalytically active with activities similar to those of free rCcP. We demonstrate that the Michaelis constants determined from steady-state kinetics studies are in good agreement with published values for the equilibrium dissociation constants of the 1:1 and 2:1 noncovalent complexes, K_{D1} and K_{D2} , respectively, and can be used as measures of binding affinity between cytochrome *c* and CcP. The data provide evidence for significant electrostatic repulsion between bound cytochrome *c* molecules on the surface of CcP at low ionic strength with the interaction energy diminishing with increasing ionic strength. Above 100 mM ionic strength, the interaction energy is effectively zero.

MATERIALS AND METHODS

Synthesis of the CcP/Cytochrome *c* Covalent Complexes. The starting clones containing the genes for CcP and yeast iso-1 cytochrome *c*, mutagenesis techniques, protein expression, and protein purification have been previously described (16). Both wild-type CcP and yeast iso-1 cytochrome *c* contain single cysteine residues, Cys-128 in CcP and Cys-102 in yeast iso-1 cytochrome *c*. The cysteine residues in the wild-type proteins were eliminated by conversion to Ser-128 in rCcP and Thr-102 in recombinant cytochrome *c* prior to constructing specifically engineered cysteine sites in the two proteins. The conversion of the wild-type cysteine residues to hydroxy containing amino acid residues eliminates the possibility of making undesired disulfide bonds during the synthesis of the covalent complexes. Four rCcP mutants were constructed: rCcP(V5C), rCcP(K12C), rCcP(N78C), and rCcP(K264C); each of these rCcP mutants contain the C128S alteration. A single cytochrome *c* mutant was constructed, cytochrome *c*(K79C), a mutation that also contains the C102T change.

The synthesis of the covalent complexes was performed in a manner similar to that described by Papa and Poulos (17). Slight modifications to the Papa–Poulos procedure were developed to improve the yield, and these modifications have been described (16). Four covalent complexes were synthesized, and these are designated V5C/K79C, K12C/K79C, N78C/K79C, and K264C/K79C. The complex names give the mutational designation in rCcP followed by the mutational designation in cytochrome *c*.

The covalent complexes were separated from the synthetic reaction mixture by chromatography using a carboxymethyl-cellulose (Whatman CM52) column (1 × 10 cm) as previously described (16). The starting buffer was O₂-saturated 25 mM ammonium acetate. Stepwise elution with increasing concentrations of ammonium acetate was used to recover fractions containing the covalent complex. Pooled fractions containing the covalent complex were dialyzed against 4 to 5 changes of deionized water at 4 °C, lyophilized, and stored at −20 °C until used.

SDS–PAGE Analysis. Sodium dodecyl sulfate–polyacrylamide gel electrophoresis (SDS–PAGE) was performed using a PhastSystem from Pharmacia LKB Biotechnology AB, Uppsala, Sweden. Proteins were incubated at room

temperature for 15 min in a 10 mM Tris/HCl buffer at pH 8, containing 2.5% SDS and 1 mM EDTA. To preserve the covalent disulfide cross-links, the denaturing buffer did not contain disulfide bond reducing agents. Protein samples were loaded onto a PhastGel gradient 10–15 pre-cast gel along with standard molecular weight markers. SDS buffer strips were used during electrophoresis. The gels were stained with Coomassie blue.

Protein Concentration Determination. Spectra of all proteins were acquired using either a Varian/Cary Model 3E spectrophotometer or a Hewlett-Packard Model 8452A diode array spectrophotometer. The spectra were used to determine protein concentration using the extinction coefficients at the Soret maximum. An extinction coefficient of 98 mM^{−1} cm^{−1} at the Soret maximum (408 nm) was used to determine the concentration of rCcP and its mutants. Extinction coefficients of 118 mM^{−1} cm^{−1} (408 nm) and 150 mM^{−1} cm^{−1} (414 nm) were used to determine the concentration of oxidized and reduced recombinant yeast iso-1 cytochrome *c*(C102T) and its mutants, respectively (16).

Hydrogen Peroxide Concentration. Hydrogen peroxide was reagent grade 30% (v/v) purchased from Aldrich Chemical Co., Inc. Hydrogen peroxide stock solutions were standardized by titration with cerium(IV) sulfate (18).

Steady-State Kinetic Studies. Steady-state kinetic studies were performed at pH 7.5 in potassium phosphate buffers of varying ionic strength. Buffer, cytochrome *c*, and enzyme were thermally equilibrated at 25 °C in the spectrophotometer, initial absorbance readings made, and then the reaction initiated by the addition of hydrogen peroxide. Initial velocities, v_0 , were determined as a function of yeast iso-1 ferrocycytochrome *c*(C102T) concentration (generally 1 to 100 μM) at constant hydrogen peroxide (200 μM). Initial velocities were calculated by measuring the time-dependent change in absorbance upon oxidation of ferrocycytochrome *c* at multiple wavelengths using a Hewlett-Packard Model 8452A diode array spectrophotometer. Five different wavelengths, generally chosen from 314, 362, 418, 448, 468, 478, 548, 564, and 574 nm depending upon the substrate concentration, were used to calculate the initial velocity at each set of experimental conditions using eq 1.

$$\frac{v_0}{e_0} = \frac{1}{2(1 - f_{ox})\Delta\epsilon} \Delta A / \Delta t \quad (1)$$

The symbols in eq 1 include the initial velocity, v_0 , the total enzyme concentration, e_0 , the change in absorbance with time, $\Delta A / \Delta t$, and the difference in extinction coefficient, $\Delta\epsilon$, between oxidized and reduced yeast iso-1 cytochrome *c*(C102T). Samples of the substrate may contain small amounts of oxidized cytochrome *c* that inhibit the reaction; f_{ox} is the fraction of oxidized cytochrome *c* in the substrate and is used to make small corrections to the initial velocity. The factor of 2 in the denominator converts cytochrome *c* turnover to enzyme turnover because two cytochrome *c* molecules are oxidized per enzymatic cycle.

RESULTS AND DISCUSSION

Design and Synthesis of the Covalent Complexes. In a previous publication (16), we reported on the synthesis and characterization of a covalent cytochrome *c*/CcP complex

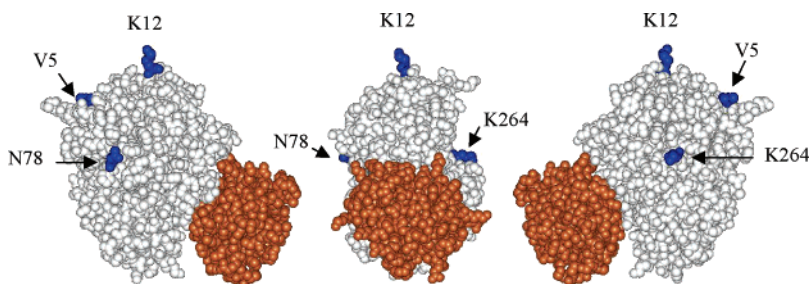


FIGURE 1: Yeast iso-1 cytochrome *c*/CcP complex (9). Yeast cytochrome *c* is shown in red, CcP is shown in white, and the residues in CcP that were individually converted to cysteine residues are shown in blue. (Center) Space-filling rendering of the complex with cytochrome *c* in front of the CcP molecule. This view defines the front face of CcP. The primary cytochrome *c*-binding site is located on the lower half of the front face of CcP. Three of the four CcP residues that are converted to cysteine residues can be seen in this view: Lys-12, Asn-78, and Lys-264. (Right-hand side) A 90° clockwise rotation of the central Figure about the vertical axis exposes the right face of the CcP molecule. Val-5, on the back side of CcP, can be seen as well as the relative locations of Lys-12 and Lys-264. (Left-hand side) A 90° counter-clockwise rotation of the central Figure about the vertical axis exposes the left face of CcP. Val-5, Lys-12, and Asn-78 are seen in this view.

in which the covalently bound cytochrome *c* blocked the primary binding site, the cytochrome *c*-binding site identified in the crystallographic structure of the noncovalent complex between yeast iso-1 cytochrome *c* and CcP (9). This complex was completely inactive, and we concluded that only cytochrome *c* bound at the primary binding site could transfer electrons to the oxidized CcP intermediates during catalytic turnover. The catalytic activity of CcP measures the reaction occurring at the primary binding site.

In this study, our objective was to determine the effect of cytochrome *c* molecules covalently bound to the surface of CcP at locations other than the primary binding site on the reactions occurring at the primary site. We designed four complexes that have the covalently bound cytochrome *c* sufficiently far from the primary binding site to minimize the steric inhibition of free cytochrome *c* binding at the primary site. All of the experimental evidence indicates that free cytochrome *c* only binds to the primary binding site in these covalent complexes.

Figure 1 shows the covalent attachment sites on CcP relative to the primary binding site, and it also defines the front face, the right-side, the left-side, and the back-side of CcP. The V5C/K79C complex has a yeast cytochrome *c* covalently attached to the back-side of CcP, located ~180° from the primary cytochrome *c* binding site, as far from the primary binding site as possible on the surface of CcP. The other three complexes have the covalently bound cytochrome *c* located ~90° from the primary binding site.

The four covalent complexes were synthesized as previously described (16, 17). Yields of the four complexes were similar to that reported for the E290C/K73C complex (16). SDS-PAGE analysis of overloaded gels of the covalent complexes showed small amounts of unreacted rCcP and cytochrome *c* in the purified samples. This is consistent with the results found for the E290C/K73C complex reported previously (16), where it was shown that small amounts of unreacted rCcP and recombinant yeast iso-1 cytochrome *c* co-purify with the covalent complexes.

Steady-State Kinetics of the Covalent Complexes at 10 mM Ionic Strength. Figure 2 shows the initial velocities for the oxidation of recombinant yeast iso-1 ferrocycytochrome *c*(C102T) by hydrogen peroxide as catalyzed by the V5C/K79C covalent complex as a function of the ferrocycytochrome *c* concentration. Figure 2 includes similar data for rCcP catalysis for reference. It is readily apparent that the V5C/

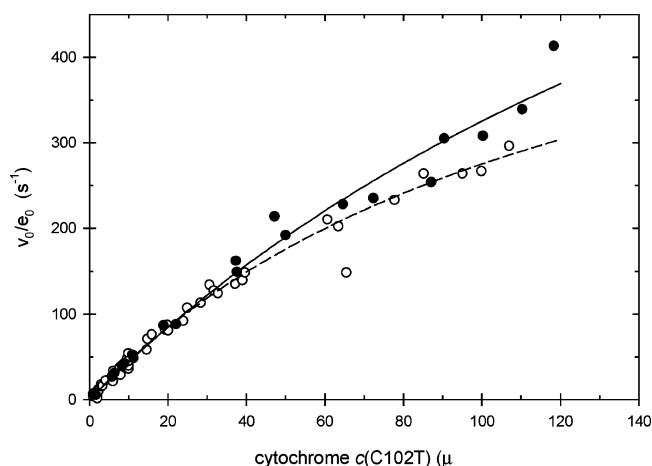


FIGURE 2: Steady-state velocities for recombinant yeast iso-1 ferrocycytochrome *c*(C102T) oxidation as a function of the cytochrome *c* concentration at 10 mM ionic strength at pH 7.5 and [H₂O₂] = 200 μM. The reaction is catalyzed either by rCcP (○) or the V5C/K79C covalent complex (●).

K79C covalent complex is as catalytically active as rCcP itself under these conditions. Although the data formally fit the Michaelis–Menten equation, there is insufficient curvature in the plots to obtain accurate values of both the Michaelis constant and the maximum velocity. This is a direct indication that the interaction between enzyme and substrate is very weak under these experimental conditions and that only a small fraction of the enzyme is converted to the enzyme–substrate complex during the steady-state turnover, even at the highest substrate concentration used in the experiments.

The most accurate steady-state parameter that can be obtained from the 10 mM ionic strength data is the limiting slope of the plot of velocity versus ferrocycytochrome *c* concentration at low substrate concentration. A modified form of the Michaelis–Menten equation was used to fit the data, eq 2,

$$\frac{v_0}{e_0} = \frac{k_{bi}}{1 + \frac{[c^{2+}]}{K_M}} \quad (2)$$

where $k_{bi} = V_M/(e_0 \cdot K_M)$. k_{bi} has units of an apparent bimolecular rate constant and is the initial slope of a plot of

Table 1: Steady-State Parameters for the Oxidation of Recombinant Yeast Iso-1 Ferrocycytochrome *c* by rCcP and Four Cytochrome *c*/CcP Covalent Complexes at Both 10 and 100 mM Ionic Strength^a

catalyst	10 mM ionic strength			100 mM ionic strength	
	k_{bi} ($\mu\text{M}^{-1} \text{s}^{-1}$)	K_M (μM)	k_{cat} (s^{-1})	K_M (μM)	k_{cat} (s^{-1})
rCcP	4.8 ± 0.2	130 ± 20	630 ± 50	2.1 ± 0.2	640 ± 10
V5C/K79C	4.6 ± 0.4	250 ± 80	1100 ± 300	2.7 ± 0.3	410 ± 10
K12C/K79C	4.4 ± 0.3	240 ± 50	1000 ± 200	2.6 ± 0.4	330 ± 10
N78C/K79C	4.1 ± 0.7	170 ± 100	680 ± 290	2.3 ± 0.3	320 ± 10
K264C/K79C	4.0 ± 0.8	170 ± 110	690 ± 330	3.7 ± 0.6	470 ± 20

^a Substrate: recombinant yeast iso-1 ferrocycytochrome *c*(C102T); $[\text{H}_2\text{O}_2] = 200 \mu\text{M}$; potassium phosphate buffer at pH 7.5 and 25 °C.

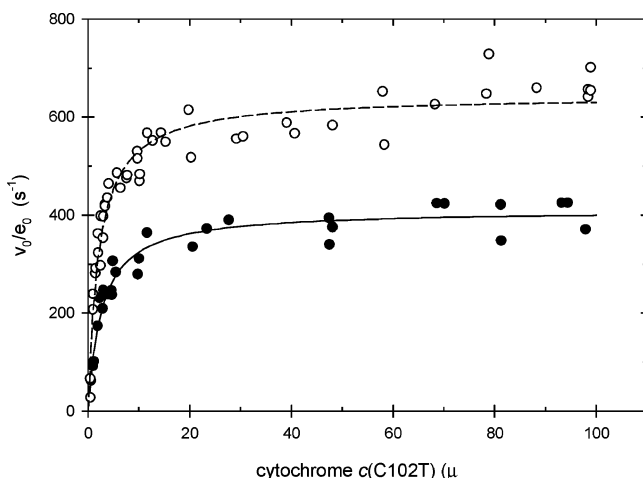


FIGURE 3: Steady-state velocities for recombinant yeast iso-1 ferrocycytochrome *c*(C102T) oxidation as a function of the cytochrome *c* concentration at 100 mM ionic strength at pH 7.5 and $[\text{H}_2\text{O}_2] = 200 \mu\text{M}$. The reaction is catalyzed either by rCcP (○) or the V5C/K79C covalent complex (●).

the normalized initial velocities versus the substrate concentration. It can be considered a lower limit to the bimolecular rate constant for the association of cytochrome *c* and the enzyme under these conditions. The value of the maximum turnover rate, $k_{cat} = V_M/e_0$, can be calculated from k_{bi} and K_M . The steady-state parameters for rCcP and the V5C/K79C covalent complex are shown in Table 1. The steady-state parameters for the other three complexes are also given in Table 1. Plots of the data for the K12C/K79C, N78C/K79C, and K264C/K79C complexes are included in the Supporting Information.

As can be seen from the data in Table 1, the initial slopes, k_{bi} , for all four covalent complexes are within the estimated experimental error of k_{bi} for rCcP. The K_M values vary by about a factor of 2, ranging from 130 μM for rCcP to 250 μM for the V5C/K79C complex. The precision of K_M is not high because all of the fitted K_M values are greater than the highest substrate concentrations used in these steady-state experiments. Likewise, the calculated maximum turnover rates, k_{cat} , vary by about a factor of 2, from 630 s^{-1} for rCcP to about 1100 s^{-1} for the V5C/K79C complex. As is to be expected, there is a strong positive correlation between the K_M and k_{cat} values.

Steady-State Kinetics of the Covalent Complexes at 100 mM Ionic Strength. Figure 3 shows the initial velocities for the oxidation of recombinant yeast iso-1 ferrocycytochrome

c(C102T) by hydrogen peroxide as catalyzed by the V5C/K79C covalent complex as a function of the ferrocycytochrome *c* concentration. Figure 3 includes similar data for rCcP catalysis for reference. Plots of the steady-state velocity data at 100 mM ionic strength for the other three complexes are included in the Supporting Information. At 100 mM ionic strength, the apparent binding affinity of cytochrome *c* to CcP is much higher than that at 10 mM ionic strength, K_M values between 2 and 4 μM at 100 mM ionic strength compared to $K_M > 100 \mu\text{M}$ at 10 mM ionic strength. In the case of the wild-type yeast CcP, the Michaelis constants have been associated with the binding of cytochrome *c* to the primary binding site at 100 mM ionic strength and the binding of cytochrome *c* to a secondary binding site at 10 mM ionic strength (19). At 100 mM ionic strength, the curvature in the velocity/substrate plots is sufficiently great that accurate values for both K_M and k_{cat} can be obtained, and these are included in Table 1. Both K_M and k_{cat} for the covalent complexes are within a factor of 2 of the corresponding parameters for rCcP.

All four covalent complexes have the primary cytochrome *c*-binding site accessible to the substrate, and substrate turnover is efficient. There is a systematic trend in the data, with the k_{cat} values for the complexes slightly lower than k_{cat} for rCcP and the K_M values for the complexes slightly larger than the K_M value for rCcP. Another interesting observation is that the k_{bi} values at 100 mM ionic strength vary much less than those of either K_M or k_{cat} . The k_{bi} values range from $1.3 \times 10^8 \text{ M}^{-1} \text{s}^{-1}$ for both the K12C/K79C and K264C/K79C complexes to $1.6 \times 10^8 \text{ M}^{-1} \text{s}^{-1}$ for rCcP. These apparent bimolecular rate constants are approaching the diffusion limit for association rate constants (20) suggesting that the binding of cytochrome *c* to the primary binding site on CcP is very efficient at the higher ionic strength.

Ionic Strength Dependence of K_M for the V5C/K79C Complex. It has previously been shown (19) that plots of the steady-state initial velocities as a function of the yeast iso-1 ferrocycytochrome *c* concentration for wild-type yeast CcP are generally biphasic and can be empirically fit to an equation that is the sum of two Michaelis–Menten terms. The high-affinity Michaelis constant, K_{M1} , is related to substrate dissociation from the 1:1 cytochrome *c*/CcP complex, and the low-affinity Michaelis constant, K_{M2} , is related to dissociation from the 2:1 complex. Because of the ionic strength dependence of cytochrome *c* binding to both the primary and secondary binding sites on yCcP, the initial velocity plots revert to simple, single term Michaelis–Menten plots at low ($\leq 20 \text{ mM}$) and high ($\geq 100 \text{ mM}$) ionic

Table 2: Steady-State Parameters for the V5C/K79C Covalent Complex at Various Ionic Strengths^a

ionic strength (mM)	k_{bi} ($\mu\text{M}^{-1}\text{s}^{-1}$)	K_M (μM)	k_{cat} (s^{-1})
10	4.6 ± 0.4	250 ± 80	1100 ± 300
20	3.2 ± 0.2	120 ± 20	390 ± 40
30	3.4 ± 0.3	210 ± 80	740 ± 220
50	6.4 ± 1.2	56 ± 19	360 ± 60
70	53 ± 8	4.6 ± 0.8	240 ± 10
100	150 ± 10	2.7 ± 0.3	410 ± 10

^a Substrate: recombinant yeast iso-1 ferrocycytochrome *c*(C102T); $[\text{H}_2\text{O}_2] = 200 \mu\text{M}$; potassium phosphate buffer at pH 7.5 and 25 °C.

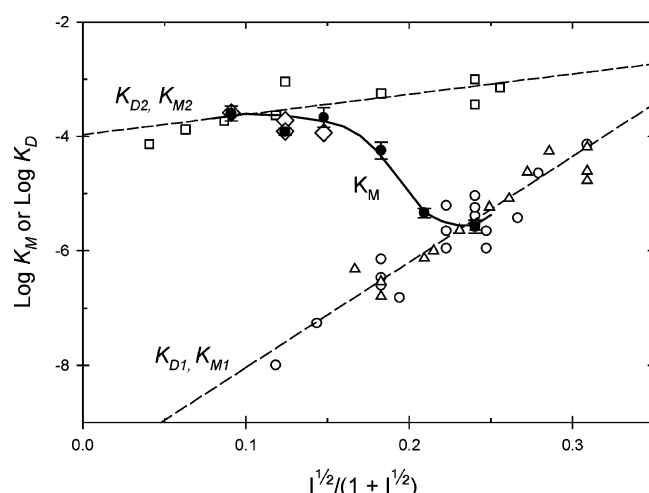


FIGURE 4: Variation of K_M (●) for the V5C/K79C covalent complex as a function of ionic strength. Published data are included for reference. The lower linear plot includes published values of K_{D1} (○) for the yeast iso-1 cytochrome *c*/CcP complex. The K_{D1} values include data collected between 18 and 200 mM ionic strength, between pH 5.5 and 7.0, and for complexes formed using either ferri- or ferrocycytochrome *c* (11–13). Michaelis constants for the high-affinity phase, K_{M1} (△), of the steady-state oxidation of yeast iso-1 ferrocycytochrome *c* catalyzed by yCcP (19) and CcP(MI) (23) are included. The upper linear plot includes values for K_{D2} (□) obtained between 1.8 mM and 118 mM ionic strength, between pH 6 and 7, using proton uptake measurements (11) and dynamic fluorescence quenching of zinc-modified CcP (7, 14, 15). Michaelis constants for the low-affinity phase, K_{M2} (◇), of the steady-state oxidation of yeast iso-1 ferrocycytochrome *c* catalyzed by yCcP (19) and CcP(MI) (23) are included.

strengths. The low ionic strength data only monitor properties of the 2:1 complex, whereas the high ionic strength data only reflect properties of the 1:1 complex. As shown in Figures 2, 3, and S1 (Supporting Information), the steady-state velocity plots for rCcP and the four covalent complexes fit the simple Michaelis–Menten equation at both 10 and 100 mM ionic strength.

The V5C/K79C complex was chosen for a more complete study of the ionic strength dependence of the steady-state parameters. The initial velocities for the V5C/K79C complex could be fit to the simple Michaelis–Menten equation at all ionic strengths between 10 and 100 mM. The steady-state parameters, k_{bi} , K_M , and k_{cat} , for the V5C/K79C complex at different ionic strengths are shown in Table 2. Figure 4 shows a plot of K_M for the V5C/K79C complex as a function of ionic strength along with reference data from the literature (21).

Some comment on the reference data shown in Figure 4 is useful for a full understanding of the significance of the ionic strength dependence of the K_M values for the V5C/K79C complex. Equilibrium dissociation constants, K_{D1} , for the 1:1 yeast iso-1 cytochrome *c*/CcP complex are shown by the open circles in the lower plot in Figure 4. These data include all published values for K_{D1} between pH 5.5 and 7.0 (11–13) because the pH dependence of K_{D1} is small relative to the logarithmic scale used in Figure 4. The most extensive data set suggests that K_{D1} varies by about a factor of 2 over the pH range 6.0 to 7.5 at 50 mM ionic strength (11). Most of the data are for the binding of the oxidized form of the yeast cytochrome, but the plot includes three data points for the reduced cytochrome *c*/CcP complex. The binding affinity for reduced cytochrome *c* is about 3-fold weaker than that for oxidized yeast iso-1 cytochrome *c*, again small, relative to the range of K_{D1} shown in Figure 4. The dashed line through the lower plot is generated by linear least-square regression of the logarithm of K_{D1} as a function of the ionic strength as defined in eq 3.

$$\log K_{D1} = -9.88 + 18.43 \frac{\sqrt{I}}{1 + \sqrt{I}} \quad (3)$$

The experimental K_{D1} values span a range >7000-fold between 18 and 200 mM ionic strength. Equation 3 predicts the values of K_{D1} within a factor of 2 in most cases with the average RMS deviation $\pm 60\%$ of the mean value.

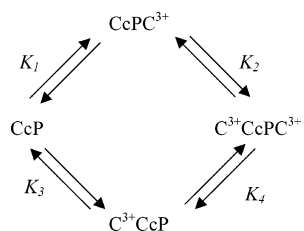
The open triangles shown in the lower plot of Figure 4 are Michaelis constants for the high-affinity phase, K_{M1} , of the steady-state oxidation of yeast iso-1 ferrocycytochrome *c* as catalyzed by wild-type yeast CcP (19) and by recombinant CcP(MI) (23). The data were collected at both pH 6.0 and 7.5 and between 40 and 200 mM ionic strength. As can be seen in Figure 4, the available K_{M1} values cluster around the K_{D1} values, and one can assume that the Michaelis constants are reasonable measures for the binding of yeast iso-1 cytochrome *c* to CcP. Comparing experimental values of K_{M1} with values of K_{D1} calculated from eq 3 indicates that K_{M1} is only about 10% larger than K_{D1} on average, within the experimental error of both measurements.

There are relatively few quantitative values for K_{D2} and K_{M2} in the literature. The open squares shown in the upper plot of Figure 4 are published values for K_{D2} (7, 11, 14, 15). The open diamonds shown in the upper plot of Figure 4 are K_{M2} values for the low-affinity phase of the steady-state oxidation of yeast iso-1 ferrocycytochrome *c* by wild-type CcP at pH 7.5 (19) and recombinant CcP(MI) at pH 6.0 (23). The K_{M2} values could only be determined between 10 and 30 mM ionic strength. Again, there is good agreement between the K_{D2} and K_{M2} values, indicating that K_{M2} is reporting the interaction of cytochrome *c* at the secondary binding site. The upper dashed line in Figure 4 was calculated from eq 4, the correlation line for the logarithm of K_{D2} as a function of ionic strength.

$$\log K_{D2} = -3.97 + 3.53 \frac{\sqrt{I}}{1 + \sqrt{I}} \quad (4)$$

Figure 4 shows the value of K_M for the V5C/K79C as a function of ionic strength. The value of K_M for the V5C/K79C complex is comparable to K_{D2} for CcP at low ionic

Scheme 1. Microscopic Model for the Binding of Cytochrome *c* to Two Unique Sites on CcP, a Primary Binding Site (Right-Hand Side) and a Secondary Binding Site (Left-Hand Side)



strength and to K_{D1} for CcP at high ionic strength. As outlined above, the Michaelis constant for the V5C/K79C complex is a direct measure of the binding of yeast iso-1 cytochrome *c*(C102T) to the primary binding site on the surface of the CcP in the covalent complex. At high ionic strength, ≥ 100 mM, the covalently bound cytochrome has little influence on the binding of exogenous cytochrome *c* to the primary binding site. The binding affinity for exogenous cytochrome *c* is essentially identical for both V5C/K79C and CcP. Under these conditions, there is no interaction between the two bound cytochromes, whether the cytochromes are bound covalently or noncovalently.

At low ionic strength, ≤ 20 mM, there is strong electrostatic repulsion between the covalently bound cytochrome *c* and cytochrome *c* binding to the primary site. In this case, the Michaelis constant is similar to K_{D2} . Note that in the case of the V5C/K79C complex, the Michaelis constant is measuring the binding of cytochrome *c* at the primary site of rCcP in the presence of a cytochrome *c* covalently bound at a secondary site, whereas for the noncovalent complex, K_{D2} is a measure of the binding of cytochrome *c* to a secondary site in the presence of a noncovalently bound cytochrome at the primary binding site.

Model for the Yeast Cytochrome *c*/CcP Interactions. The model for cytochrome *c* binding to CcP that emerges from these results is one of unique interacting sites. The primary binding site has a higher intrinsic affinity for cytochrome *c* than the secondary site, and there are strong interactions between sites at low ionic strength. The interaction energy is modulated by ionic strength and effectively goes to zero at ≥ 100 mM ionic strength. The binding model is shown in Scheme 1, where the binding of cytochrome *c* to the primary binding site is represented by placing the symbol for cytochrome *c* to the right-hand side of CcP and for binding at a secondary site, by placing the symbol on the left-hand side of the CcP. K_1 , K_2 , K_3 , and K_4 represent the microscopic or site-specific constants. Thus K_1 represents the microscopic equilibrium dissociation constant for the 1:1 complex with the cytochrome *c* bound at the primary binding site and K_3 the dissociation constant for the 1:1 complex in which cytochrome *c* is bound at a secondary site. K_2 represents the equilibrium dissociation constant for the 2:1 complex in which cytochrome *c* dissociates from the secondary site, and K_4 represents the dissociation of cytochrome *c* from the primary binding site in the 2:1 complex. For an in-depth description of this binding model see ref 24 (24).

The relationship between the microscopic equilibrium constants shown in Scheme 1 and the observed equilibrium dissociation constants are given by eqs 5 and 6.

$$K_{D1} = \frac{K_1 K_3}{K_1 + K_3} \quad (5)$$

$$K_{D2} = K_2 + K_4 \quad (6)$$

The crystal structures of CcP and the 1:1 yeast cytochrome *c*/CcP noncovalent complex (4, 9) show no significant conformational differences in CcP upon binding of yeast cytochrome *c*. This suggests that the intrinsic binding affinities of the primary and secondary binding sites are not affected by complex formation and that K_2 and K_4 are only affected by electrostatic repulsion between cytochromes binding at the two sites in the 2:1 complex. Equations 7 and 8 show the relationships between K_1 and K_4 and between K_2 and K_3 , respectively.

$$K_4 = K_1 e^{\Delta G_i/RT} \quad (7)$$

$$K_2 = K_3 e^{\Delta G_i/RT} \quad (8)$$

At ionic strengths ≥ 100 mM, K_M is numerically equal to K_{D1} , indicating that covalently bound cytochrome *c* in the covalent complex has essentially no effect on the binding of cytochrome *c* at the primary binding site. The interaction energy, ΔG_i , is effectively zero, and $K_2 = K_3$ and $K_4 = K_1$. Under high ionic strength conditions, the microscopic constants can be calculated from the observed equilibrium dissociation constants. Using eqs 3–8, with the stipulation that ΔG_i is zero, one can determine that $K_1 = K_4 = 3.5 \mu\text{M}$ and $K_2 = K_3 = 750 \mu\text{M}$ at 100 mM ionic strength. The affinity for yeast iso-1 cytochrome *c* binding at the primary site is greater than 200 times the binding affinity at any secondary site in the formation of 1:1 complexes, and less than 0.5% of the 1:1 complexes in solution have cytochrome *c* bound at a secondary site. The upper pathway in Scheme 1 is a good representation of the binding of cytochrome *c* to CcP with the lower pathway making a negligible contribution.

As the ionic strength is decreased, electrostatic repulsion between cytochrome *c* bound at the primary binding site weakens binding at the secondary binding site relative to binding at the primary site, and at 10 mM ionic strength, there is a difference of about 35000 in binding affinity, that is, $K_1 \cong K_{D1} = 6.2 \text{ nM}$ and $K_2 \cong K_{D2} = 220 \mu\text{M}$.

The data for the V5C/K79C complex can be used to calculate the minimum interaction energy as a function of ionic strength. $K_{D1} \cong K_1$ represents the intrinsic binding at the primary binding site as a function of ionic strength, whereas K_M for the V5C/K79C complex represents the binding of cytochrome *c* to the primary binding site in the presence of a covalently bound cytochrome *c*, positioned as far as possible from the primary binding site on the surface of CcP. Equation 9 can be used to calculate ΔG_i at any ionic strength for which K_M has been determined. At 10 mM ionic strength, the interaction energy is +6.3 kcal/mol.

$$\Delta G_i = 2.303RT \left(\log K_M + 9.88 - 18.43 \frac{\sqrt{I}}{1 + \sqrt{I}} \right) \quad (9)$$

The ionic strength modulates the electrostatic repulsion between the bound cytochromes in the 2:1 complex, and this provides a rationale for the observation that K_{D2} is not as

dependent upon the ionic strength as K_{D1} (Figure 4 and eqs 3 and 4). The intrinsic binding constant at both the primary and secondary binding sites is determined in large part by the electrostatic attraction between the negatively charged CcP and the positively charged cytochrome *c*. At pH 7.5, the net charge on CcP is about -10 (25) and about $+5$ on cytochrome *c* (26), leading to a very large slope ($+18.43$) in the plot of $\log K_{D1}$ as a function of ionic strength (Figure 4 and eq 3). However, the intrinsic electrostatic attraction of the secondary binding site is largely compensated by the electrostatic repulsion from the cytochrome bound at the primary site, decreasing the ionic strength dependence of $\log K_{D2}$ by a factor of 5 (eq 4).

One of the initial objectives of this project was to determine if the covalent complexes could give some information concerning the location of potential secondary binding sites on the basis of the assumption that the interaction energy between covalently bound cytochrome *c* and cytochrome *c* binding at the primary site would depend upon the location of the covalently attached cytochrome *c*. However, the data at 10 mM ionic strength (Table 1) indicate that the interaction between the covalently bound cytochromes and cytochrome *c* binding at the primary site is essentially the same for all four complexes, regardless of the location of the covalently bound cytochrome *c*.

CONCLUSIONS

The Michaelis constants from steady-state kinetic studies of the CcP-catalyzed oxidation of yeast iso-1 ferrocycytochrome *c* by hydrogen peroxide agree quite well with the equilibrium dissociations constants for the 1:1 and 2:1 yeast iso-1 cytochrome *c*/CcP complexes and can be used as measures of the interaction between cytochrome *c* and CcP. The binding model for yeast cytochrome *c* and CcP can be described as a unique two-site interacting model in which the primary binding site for cytochrome *c* on the surface of CcP has an affinity for the yeast cytochrome that is at least 200-times greater than that of the secondary site. The observed equilibrium dissociation constant, K_{D1} , is essentially a specific site constant and represents the dissociation of cytochrome *c* from the primary site at all ionic strengths. Likewise, K_{D2} represents the dissociation of cytochrome *c* from a secondary binding site in the 2:1 complex. There is strong electrostatic repulsion between cytochrome *c* molecules bound at the two sites at low ionic strength, but the electrostatic interaction energy decreases with increasing ionic strength and is negligible above 100 mM ionic strength.

ACKNOWLEDGMENT

We thank Professor James Satterlee, Washington State University for providing the plasmid containing the gene for rCcP and Professor Gary Pielak, University of North Carolina, Chapel Hill for providing the plasmid containing the yeast iso-1 cytochrome *c*(C102T) and heme lyase genes.

SUPPORTING INFORMATION AVAILABLE

Plots of the steady-state velocities as a function of the yeast ferrocycytochrome *c* concentration for the K12C/K769C, N78C/K79C, and K264/K79C covalent complexes at both

10 and 100 mM ionic strength. This material is available free of charge via the Internet at <http://pubs.acs.org>.

REFERENCES

- Yonetani, T., and Ohnisi, T. (1966) Cytochrome *c* peroxidase, a mitochondrial enzyme of yeast, *J. Biol. Chem.* **241**, 2983–2984.
- Yonetani, T. (1966) Studies on cytochrome *c* peroxidase IV. A comparison of peroxide-induced complexes of horseradish and cytochrome *c* peroxidases, *J. Biol. Chem.* **241**, 2562–2571.
- Poulos, T. L., Freer, S. T., Alden, R. A., Edwards, S. L., Skogland, U., Takio, K., Eriksson, B., Xuong, N., Yonetani, T., and Kraut, J. (1980) The crystal structure of cytochrome *c* peroxidase, *J. Biol. Chem.* **255**, 575–580.
- Finzel, B. C., Poulos, T. L., and Kraut, J. (1984) Crystal structure of yeast cytochrome *c* peroxidase refined at 1.7-Å resolution, *J. Biol. Chem.* **259**, 13027–13036.
- Poulos, T. L., and Kraut, J. (1980) The stereochemistry of peroxidase catalysis, *J. Biol. Chem.* **255**, 8199–8205.
- Erman, J. E., Vitello, L. B., Miller, M. A., Shaw, A., Brown, K. A., and Kraut, J. (1993) Histidine 52 is a critical residue for rapid formation of cytochrome *c* peroxidase compound I, *Biochemistry* **32**, 9798–9806.
- Nocek, J. M., Zhou, J. S., De Forest, S., Priyadarshi, S., Beratan, D. N., Onuchic, J. N., and Hoffman, B. M. (1996) Theory and practice of electron transfer within protein-protein complexes: application to the multidomain binding of cytochrome *c* by cytochrome *c* peroxidase, *Chem. Rev.* **96**, 2459–2489.
- Bendal, D. S. (1996) *Protein Electron Transfer*, Bios Scientific Publishers, Oxford, England.
- Pelletier, H., and Kraut, J. (1992) Crystal structure of a complex between electron transfer partners, cytochrome *c* peroxidase and cytochrome *c*, *Science* **258**, 1748–1755.
- Mathews, F. S., Mauk, A. G., and Moore, G. R. (2000) Protein-Protein Complexes Formed by Electron Transfer Proteins, in *Protein-Protein Recognition* (Kleanthous, C., Ed.) pp 60–101, Oxford University Press, Oxford, England.
- Mauk, M. R., Ferrer, J. C., and Mauk, A. G. (1994) Proton linkage in formation of the cytochrome *c*-cytochrome *c* peroxidase complex: electrostatic properties of the high- and low-affinity cytochrome *c* binding sites on the peroxidase, *Biochemistry* **33**, 12609–12614.
- Wang, X., and Pielak, G. J. (1999) Equilibrium thermodynamics of a physiologically-relevant heme-protein complex, *Biochemistry* **38**, 16876–16881.
- Morar, A. S., Wang, X., and Pielak, G. J. (2001) Effects of crowding by mono-, di-, and tetrasaccharides on cytochrome *c* peroxidase binding: Comparing experiment to theory, *Biochemistry* **40**, 281–285.
- Stemp, E. D. A., and Hoffman, B. M. (1993) Cytochrome *c* peroxidase binds two molecules of cytochrome *c*: evidence for a low-affinity, electron-transfer-active site on cytochrome *c* peroxidase, *Biochemistry* **32**, 10848–10865.
- Zhou, J. S., and Hoffman, B. M. (1994) Stern-Volmer in reverse: 2:1 stoichiometry of the cytochrome *c*-cytochrome *c* peroxidase electron transfer complex, *Science* **265**, 1693–1696.
- Nakani, S., Viriyakul, T., Mitchell, R., Vitello, L. B., and Erman, J. E. (2006) Characterization of a covalently-linked yeast cytochrome *c*/cytochrome *c* peroxidase complex: Evidence for a single, catalytically-active cytochrome *c* binding site on cytochrome *c* peroxidase, *Biochemistry* **45**, 9887–9893.
- Papa, H. S., and Poulos, T. L. (1995) Site-specific crosslinking as a method for studying intramolecular electron transfer, *Biochemistry* **34**, 6573–6580.
- Kolthoff, I. M., and Belcher, R. (1957) Hydrogen Peroxide, in *Volumetric Analysis*, Vol. 3, pp 75–76, Interscience, New York.
- Matthis, A. L., and Erman, J. E. (1995) Cytochrome *c* peroxidase-catalyzed oxidation of yeast iso-1 ferrocycytochrome *c* by hydrogen peroxide: Ionic strength dependence of the steady-state parameters, *Biochemistry* **34**, 9985–9990.
- Hague, D. N. (1971) *Fast Reactions*, Wiley-Interscience, London.
- Erman, J. E., and Vitello, L. B. (2002) Yeast cytochrome *c* peroxidase: mechanistic studies via protein engineering, *Biochim. Biophys. Acta* **1597**, 193–220.

22. Yonetani, T., and Ray, G. S. (1966) Studies on cytochrome *c* peroxidase: III Kinetics of the peroxidatic oxidation of ferrocytochrome *c* catalyzed by cytochrome *c* peroxidase, *J. Biol. Chem.* 241, 700–706.
23. Miller, M. A. (1996) A complete mechanism for steady-state oxidation of yeast cytochrome *c* by cytochrome *c* peroxidase, *Biochemistry* 35, 15791–15799.
24. Klotz, I. M. (1997) *Ligand-Receptor Energetics*, Wiley, New York.
25. Conroy, C. W., and Erman, J. E. (1978), pH titration study of cytochrome *c* peroxidase and apocytochrome *c* peroxidase, *Biochim. Biophys. Acta.* 537, 396–405.
26. Theorell, H., and Åkesson, Å. (1941) Studies on cytochrome *c*. III. Titration curves, *J. Am. Chem. Soc.* 63, 1818–1820.

BI061662P